

Turbulence suppression in free shear flows by controlled excitation

By K. B. M. Q. ZAMAN AND A. K. M. F. HUSSAIN

Department of Mechanical Engineering,
University of Houston, Texas 77004

(Received 20 November 1979)

In an attempt to explain the mechanics of turbulence suppression previously observed by us in jets under controlled excitation, the near fields of four circular jets, a plane jet and a plane mixing layer, all with laminar efflux boundary layers, have been explored through hot-wire measurements. It is shown that controlled excitation, induced acoustically as well as by vibrating ribbons, can reduce turbulence intensities in all these flows. Reduction by as much as 80% is observed, the maximum decrease occurring at about $400\theta_e$ downstream from the exit; θ_e is the initial shear-layer momentum thickness. The suppression effect is a maximum for excitation at the Strouhal number St_θ ($\equiv f\theta_e/U_e$) of about 0.017. In the jets, the turbulence suppression is observed over the range $0.75 \leq x/D \leq 8$, while for the plane mixing layer it could be detected as far downstream as $x \approx 6000\theta_e$.

The flow-fields with and without excitation for a typical case of turbulence suppression have been studied in detail. Spectra of the \tilde{u} signal and time-averaged field data indicate that excitation at $St_\theta \approx 0.017$ suppresses the formation of naturally occurring energetic vortices – an observation confirmed by flow-visualization experiments and by study of the large-scale coherent structures of the shear layer, deduced through conditional-sampling measurements. Excitation at $St_\theta \approx 0.017$ produces a rapid growth of the shear layer instability mode, and consequently, its saturation, roll-up and breakdown occurs much earlier in x than is found to occur naturally (at $St_\theta \approx 0.012$). The suppression effect is apparently a consequence of earlier transition of the shear layer vortices, which otherwise naturally grow to larger sizes and survive for larger x , as well as being due to the prevention of successive pairing of these structures.

1. Introduction

In an effort to explore the coherent structure dynamics in the circular jet near field as well as examine the universality of the results of Crow & Champagne (1971), a study of controlled acoustic perturbation of the circular jet was initiated in our laboratory in 1973. In the early stage of this study, it was observed that under certain conditions of excitation, the centre-line turbulence intensity in the jet could be suppressed to values considerably below the unexcited jet values; see Hussain & Zaman (1975; hereinafter referred to as I). This suppression effect, confirmed through repeated measurements, intrigued us for quite some time because neither did Crow & Champagne observe this effect nor could we find any explanation for it. Even though subsequently

we were to become aware† of similar observations in some contemporary investigations (Vlasov & Ginevskiy 1974; Petersen, Kaplan & Laufer 1974), the suppression effect has remained unexplored and unexplained. In this paper, we present a fairly comprehensive documentation of this phenomenon in a variety of free shear flows in addition to using the experimental evidences to develop an explanation for the mechanism involved.

Various investigators have employed acoustic excitation to study instability characteristics of initially laminar free shear flows (Sato 1959, 1960; Chanaud & Powell 1965; Wille 1963; Freymuth 1966; Becker & Massaro 1968; Miksad 1972; Hussain & Thompson 1980) or the coherent structures in the near fields of various free shear flows (Brown 1935; Crow & Champagne 1971; Chan 1974; Moore 1977; Zaman & Hussain 1977, 1980; Kibens 1979). These studies in general dealt with the excitation conditions producing augmentation of the fluctuation intensities in the flows, the condition being typically met when the excitation frequency falls within the 'sensitive range' of the basic flow.

In the course of these studies of external excitation of free shear flows, some investigators also observed suppression of turbulence intensities and noise. Vlasov & Ginevskiy (1974) observed suppression of the turbulence intensities in a circular air jet when excited at the jet Strouhal number $St_D (\equiv fD/U_e)$ of 2.75; here f is the frequency, D is the jet diameter and U_e is the jet exit speed. They found that the jet centre-line turbulence intensities decreased from the corresponding unexcited values up to a downstream distance of $x/D \cong 9$, that there was an optimum intensity of the acoustic excitation at which the suppression was the maximum, and that the effect was independent of whether the jet was sound-irradiated transversely or longitudinally. In their study of the effect of controlled excitation introduced all around the lip of a 2.54 cm diameter air jet, Petersen *et al.* (1974) observed turbulence suppression at $x/D = 4$ for $St_D \cong 3.0$ and $Re_D = 5.2 \times 10^4$. Moore (1977) has observed a small reduction in the far-field broadband noise level in circular jets with laminar and turbulent exit boundary layers, for excitation at $St_D > 1.5$ and for Mach numbers up to 0.70.

From flow visualization of a plane water jet subjected to transverse disturbances by a flapping plate, Rockwell (1972) classified the plane jet response into five 'regimes'. In one of these, namely the 'preservation regime', when the excitation frequency was somewhat above the natural breakdown frequency of the plane jet, the jet core tended to be preserved for longer lengths in the flow direction. The value of $f\lambda/U_e$ in this regime was noticeably higher than that for natural breakdown, but approached the latter at higher Reynolds numbers; λ is the wavelength.

The suppression effect was observed by us initially in a 2.54 cm jet at $St_D \cong 1.6$ (see I), and subsequently also in a 7.62 cm jet at $St_D \cong 1.6$. For the latter case, the centre-line variations of the r.m.s. total and fundamental velocity amplitudes are documented by Zaman & Hussain (1980, hereinafter referenced as II). The fact that the values of St_D for maximum suppression found by Vlasov & Ginevskiy, Petersen *et al.* and us did not coincide, was an indication that St_D was not a relevant parameter. It became clear to us that the mechanism of turbulence suppression had not been documented and that an effort to explain the associated flow physics was warranted.

The objective of this study was, therefore, to investigate if the turbulence suppres-

† Mr Dennis Bushnell of the NASA Langley Research Center brought to our notice that Vlasov & Ginevskiy observed similar suppression effect.

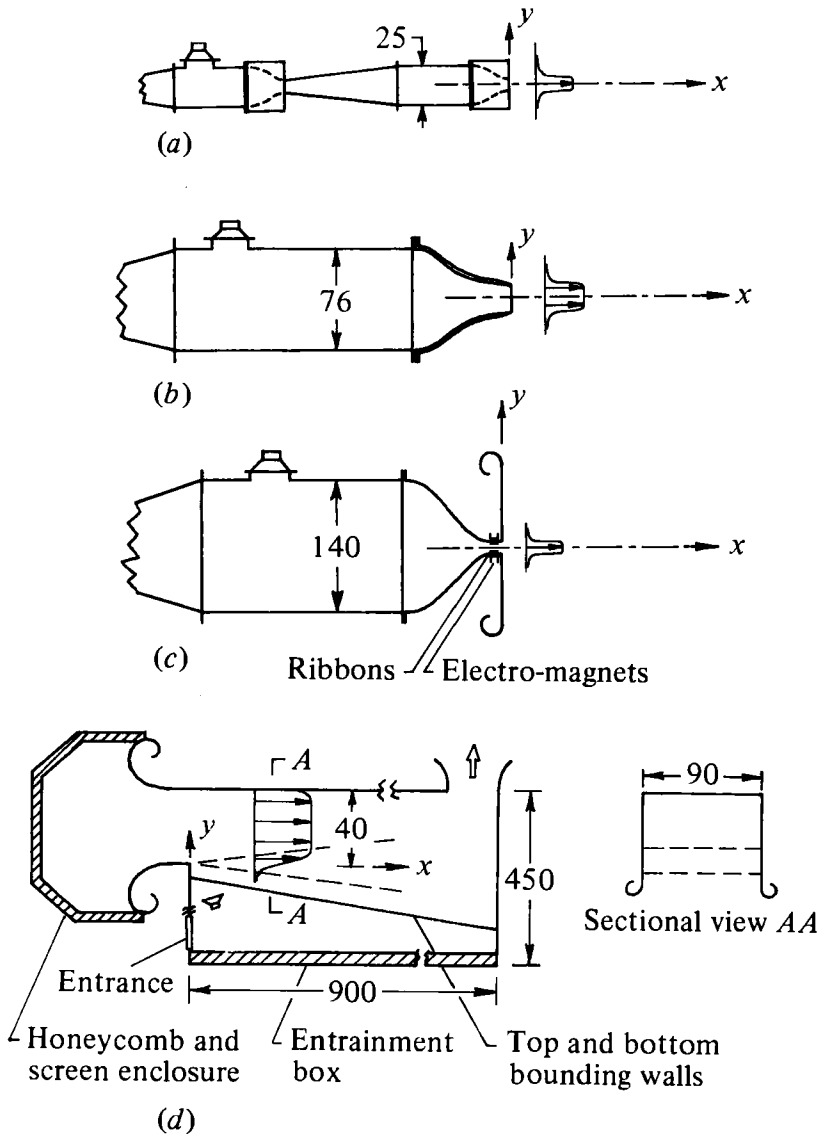


FIGURE 1. Schematics of the flow facilities. (a) 2.54 cm and 7.62 cm diameter circular jets; (b) 12.7 cm and 18 cm diameter circular jets; (c) 3.18 cm width plane jet; (d) single-stream plane free shear layer. All dimensions are in centimetres.

sion effect was unique to the axisymmetric jet and if not, document this effect in different free shear flow facilities and use the experimental data to explain the mechanism involved. It was felt that an understanding of the phenomenon could enhance the knowledge of stability mechanisms, entrainment, mixing and noise production in free shear flows, and presumably suggest a method of controlling the last.

2. Experimental procedures

The experiments were carried out in four circular air jets of diameters 2.54 cm, 7.62 cm, 12.7 cm and 18 cm, in a plane air jet of 3.18 cm width, as well as in a large single-stream plane free air mixing layer. The essential features of the facilities are schematically shown in figure 1. The two smaller circular jet flows were achieved by attaching separate nozzles to a round jet facility with a 25.4 cm diameter settling chamber; the facility is described in II. Two nozzles attached separately to a second circular jet facility with a 76 cm diameter settling chamber provided the two larger circular jet flows; see Husain & Hussain (1979) for apparatus details. The 140×3.18 cm plane jet, following a 44:1 two-dimensional contraction from a 140×140 cm settling chamber in a third flow facility, has been described by Hussain & Clark (1977). The jet facilities are located in a large air-conditioned laboratory ($30 \times 14 \times 4$ m) with controlled traffic. The jets are located sufficiently apart from each other, and they were run one at a time. Thus, the flows studied were free from significant ambient turbulence and recirculation.

The plane jet emerges normal to a 140×140 cm end plate between two 140×260 cm confining plates. The 2.54 cm and the 7.62 cm circular jets exit through the centres of 25 cm diameter end plates, but the two larger round jets have no end plates and the nozzles terminate in 20° wedges at the lip. Continuously adjustable exit speeds in each of the three facilities were obtained by centrifugal blowers driven by d.c. motors operated through full-wave rectifier controllers. Controlled acoustic excitation was induced in each jet facility by means of a loudspeaker attached to the settling chamber. In case of the plane jet, excitation studies were also done with two thin (0.1 mm thick) phosphor-bronze ribbons placed near the lips and excited with electromagnets placed outside the flow. For ribbon excitation details see Hussain & Reynolds (1970).

The single-stream plane mixing layer is formed by blowing out air from one side of an airtight room of $9 \times 4.5 \times 4$ m dimensions. A 90×40 cm rectangular cut-out on the opposite wall of that room allows air-conditioned air to flow into the room, after the air has passed through an enclosure consisting of screens, honeycombs, and a contraction. The (vertical) plane mixing layer of 90 cm span, originating from one vertical side of the cut-out is bounded between two horizontal parallel confining plates with rounded leading edges. Entrainment air is provided through a wide entrainment box running the entire length of the room; thus, vortical fluid from the mixing layer is not recirculated within the room or re-entrained. Tests show that the mixing layer is free from the effects of the side walls (see figure 1*d*) up to a downstream distance of about 4 m. For excitation, the origin of the mixing layer was irradiated by sound from a loudspeaker placed 40 cm from the midspan and away from the high-speed flow.

Note that the entrainment air merges with the primary stream at the lip orthogonally for the two small circular jets, the plane jet and the plane mixing layer but nearly parallel for the two larger circular jets. These differences are of no significance since characteristic measures of the shear layer are independent of whether the entrainment at the lip is parallel or orthogonal (Husain & Hussain 1979).

Because of the modular construction and flexible couplings, the facilities are free from any perceptible vibrations. However, the large circular jet facility has some residual fluctuations associated with the blade passage frequency, which increases with exit speed. The free-stream flow in the plane mixing layer also has very low

frequency noise (below 1 Hz) arising from background acoustic and flow disturbances. All flows had a residual free-stream turbulence intensity at the exit plane of about 0.25 %. In general, \tilde{u} -spectra at the exit planes showed that the background disturbances were distributed over a range of frequencies and did not comprise sharp, large spikes.

Data were obtained by standard (single and crossed) hot-wire techniques employing linearized constant temperature (DISA) anemometers. All the data presented were acquired in diametral planes in the round jets or in horizontal planes passing through the mid-spans of the vertical plane jet and the plane mixing layer. For the jets, the point on the centre-line in the exit plane has been used as the coordinate origin, with x denoting the axial downstream distance and y the transverse distance across the jet. Hot-wire traverses were made by automated traversing mechanisms under computer (HP 2100) control. The spectra presented represent one-dimensional longitudinal velocity spectra, $S_u(f)$, defined such that

$$\int_0^{\infty} S_u^2(f) df = \overline{u^2},$$

and were obtained by a Spectroscope SD335 real-time spectrum analyser.

For all measurements reported in this paper, the initial boundary layer was laminar, the profile and the shape factor in each case agreeing with the Blasius profile. (For careful documentation of the initial conditions in the facilities used for this study, see the cited references which describe these facilities.) For each of the jets, the exit shear layer momentum thickness (θ_e) was measured at 3 mm downstream from the lip for several exit speeds. An equation of the form $\theta_e/D = a(Re_D)^b$, least squares-fitted through the set of data, was used to obtain θ_e/D at any exit speed for each nozzle. The plane mixing layer data involved two exit speeds, namely 10 ms⁻¹ and 20 ms⁻¹; θ_e for each case was measured directly.

3. Results and discussion

The suppression effect is demonstrated in figure 2(a) by the two oscilloscope traces of the \tilde{u} -signal in the plane jet with an exit speed $U_e = 22$ ms⁻¹. For both the traces, the hot-wire probe was located at $x = 10$ cm on the centre-line ($D = 3.18$ cm). Trace (i) is for the unexcited jet flow and trace (ii) is for excitation at $f_p = 1720$ Hz with an exit excitation amplitude u'_f/U_e of 0.1 %; u'_f is the (r.m.s.) fluctuation intensity of the fundamental (f_p) measured at the exit centre-line. The corresponding traces for the 2.54 cm circular jet capturing the suppression effect are shown in figure 2(b). All traces in figure 2 have identical horizontal and vertical scales. It is evident that the excitation remarkably reduced the fluctuation amplitudes without drastically altering the spectral content (see later).

The suppression effect on the centre-line of the 2.54 cm circular jet is quantitatively shown in figure 3, where the streamwise variations of the mean velocity U_c and the longitudinal turbulence intensity u'_c for the excitation case are compared with the corresponding unexcited jet data. For this figure, the Reynolds number Re_D is 21 400, the Strouhal number St_D ($\equiv fD/U_e$) based on the diameter is 2.15, the Strouhal number St_{θ} based on the initial shear layer momentum thickness θ_e is 0.017, and the jet-exit excitation level u'_c/U_e is 1 %; u'_c is the total r.m.s. value of the longitudinal

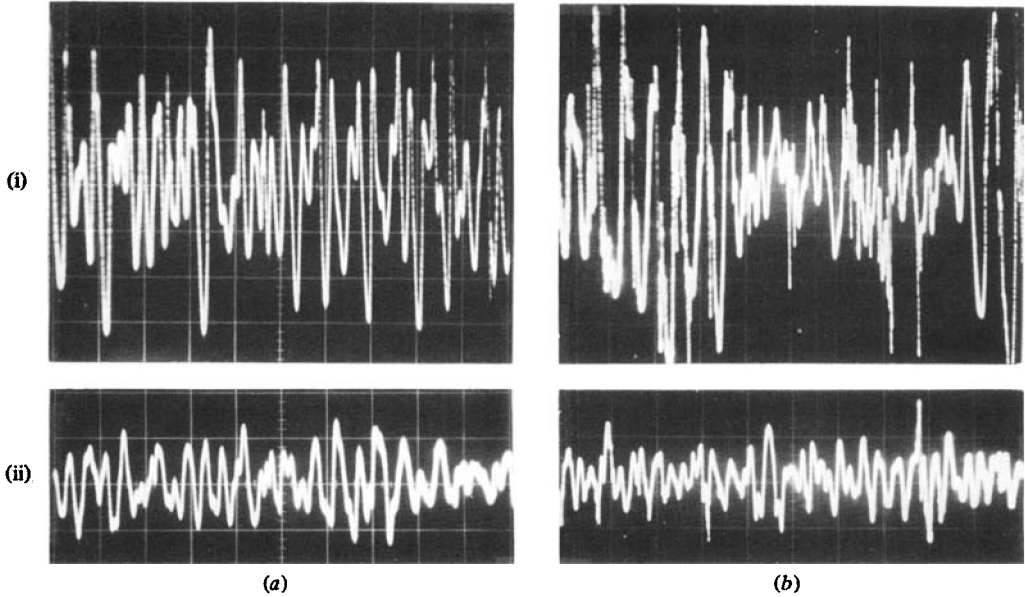


FIGURE 2. Oscilloscope traces of $\tilde{u}(t)$ signals on the centre-lines of plane and circular jets at $x = 10$ cm: (a) $D = 3.18$ cm plane jet with $U_e = 22$ ms $^{-1}$, $f_p = 1780$ Hz, $u'_j/U_e = 0.1\%$; (b) $D = 2.54$ cm circular jet with $U_e = 12.7$ ms $^{-1}$, $f_p = 1050$ Hz, $u'_j/U_e = 0.1\%$. Traces in row (i) are for unexcited flows and in (ii) for excitation; identical scales for all four traces. Each trace covers a total time period of 100 ms.

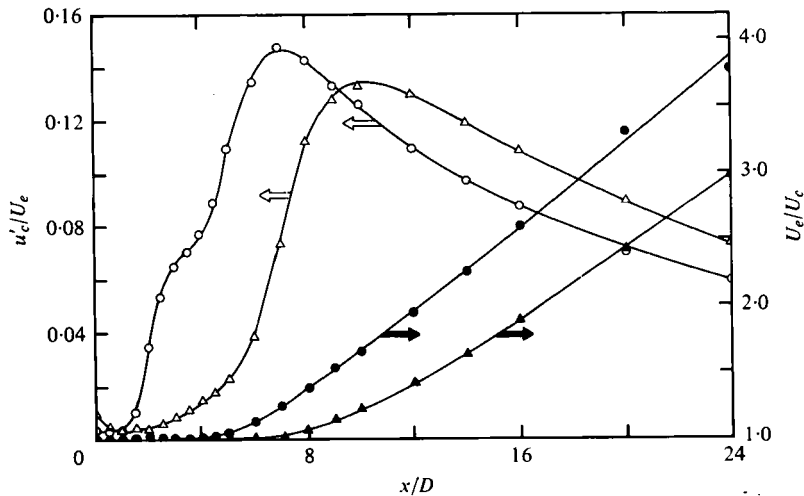


FIGURE 3. Distribution of $U_c(x)$ and $u'_c(x)$ in the 2.54 cm circular jet at $Re_D = 2.14 \times 10^4$. Triangular data points for excitation at $St_\theta = 0.017$ ($St_D = 2.15$; $u'_j/U_e = 1\%$); circular data points for corresponding unexcited jet.

velocity fluctuation $\tilde{u}(t)$ at the jet exit centre-line. Note that excitation produces reduction in u'_c in the range $0.75 \lesssim x/D \lesssim 9$ and extend the jet potential core to a longer x -range; linear upstream extrapolation of the $U_c^{-1}(x)$ data in the far field (i.e., large x -region) shows that excitation shifts the virtual origin from $x/D \cong 6$ to $x/D \cong 9.5$. Similar suppression of the centre-line turbulence intensity was also previously observed

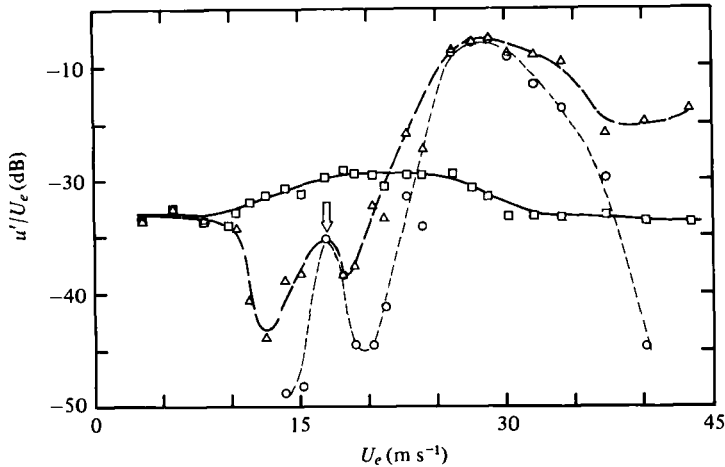


FIGURE 4. Variations with U_e of: $-\Delta-$, u'_{ex}/U_e ; $-\square-$, u'_{ux}/U_e ; $-\circ-$, $u'_{1/2f}/U_e$. Measurements at $x/D = 2$ on the centre-line of the 2.54 cm circular jet; $f_p = 1050$ Hz.

and reported for the same 2.54 cm jet at $St_D = 1.6$ and $Re_D = 12000$, and for the 7.02 cm jet at $St_D = 1.6$ and $Re_D = 41000$ (see, I, II). Vlasov & Ginevskiy's (1974) data at $St_D = 2.75$ on the centre-line turbulence intensity and mean velocity also showed trends essentially similar to those in figure 3.

3.1. The excitation condition for turbulence suppression

A systematic hot-wire survey was carried out to determine the values of excitation parameters at which maximum turbulence suppression occurs. For a fixed excitation frequency f_p , the longitudinal turbulence intensities for the excitation case (u'_{ex}) and for the corresponding unexcited case (u'_{ux}) were measured as a function of the jet exit speed U_e . (Alternatively, this survey could be carried out for a fixed U_e and varying f_p , but this scheme could not be followed for the jets because of the discrete settling chamber resonance frequencies; see II). A second (right angle) probe was used at the jet exit, such that only the prongs rather than the stem intersected the exit shear layer (so that the stem did not induce shear tone oscillations, see Hussain & Zaman 1978), in order to monitor and adjust U_e as well as the exit excitation level (u'_e/U_e). For a fixed f_p , the suppression occurred over a range of the exit speed U_e . For the 2.54 cm jet with excitation at $f_p = 1050$ Hz, the u'_{ex}/U_e and u'_{ux}/U_e data (in dB) are shown in figure 4. The r.m.s. amplitude at the subharmonic frequency ($u'_{1/2f}$) is also shown in figure 4 in order to compare the excitation conditions for the 'shear layer mode' and the 'jet-column mode' of vortex pairing (see II) with those producing the suppression effect. For these data, the hot-wire was located at $x/D = 2$ and $y = 0$ (this axial location was chosen in order to capture the $u'_{1/2f}$ -spectral component clearly); the exit excitation level was kept constant at $u'_e/U_e = 1\%$. Suppression of the turbulence intensity (i.e., $u'_{ex} < u'_{ux}$) occurs over the U_e -range of 11–20 ms^{-1} corresponding to the St_D range of 2.4–1.3 and the St_θ range of 0.021–0.009.

Careful examination of the u'_{ux} data in figure 4 reveals a wavy variation with U_e and somewhat higher values in the speed range $10 \text{ ms}^{-1} < U_e < 30 \text{ ms}^{-1}$. There is, however, no reason to expect u'_{ux}/U_e to be constant and independent of U_e for an

Jet	f_p (Hz)	u'_e/U_e †
2.54 cm circular	1520	0.7–1 %
	2480	0.9–1 %
12.7 cm circular	540	0.8 %
	1070	0.3 %
18 cm circular	856	0.3 %
3.18 cm plane	930	0.5 %
	1790	0.3 %
	2680	0.3 %

† For data at other frequencies in the jet cases (in figures 4, 5, 6 and 7) u'_e/U_e was 1 %.

TABLE 1. Excitation levels.

initially laminar jet. The u'_{ux} data in figure 4 reflect the 'footprint', on the centre-line at $x/D = 2$, of the organized motions in the shear layer. The signal on the centre-line depends on the nature and strength of the activity in the shear layer at the same x station, which may involve pairing, tearing and breakdown (Clark 1979). With increasing U_e , the most unstable wavelength will progressively decrease and at sufficiently high Re_D (i.e. U_e), the shear layer will undergo breakdown closer to the jet exit so that it is always turbulent at $x/D \cong 2$. Then, u'_{ux} on the jet centre-line at $x/D \cong 2$ can only be under the influence of the 'jet column mode' which does not change with U_e for a fixed x/D . Thus, at large U_e , u'_{ux}/U_e is expected to be independent of U_e , consistent with the data in figure 4.

The $u'_{1/2}$ amplitude variation shows two relative peaks at two exit speeds when the conditions for vortex pairing in the 'shear-layer mode' (i.e., at $St_\theta \cong 0.012$) and the 'jet-column mode' (i.e. at $St_D \cong 0.85$) are satisfied (see II). For this f_p (1050 Hz), the peak in the $u'_{1/2}$ variation corresponding to the shear layer mode of pairing (marked by an arrow) occurs within the U_e -range of 11–20 ms^{-1} over which the suppression is observed. As a result, the u'_{ex} -amplitude variation shows dual troughs, the (positive) peak in the middle being due to vortex pairing activity. This should explain similar dual troughs in the variation of u'_{ex} with U_e observed at some other excitation frequencies (discussed later). Note that even under 'stable vortex pairing' in the shear-layer mode, u'_{ex} is substantially lower than the corresponding u'_{ux} , and that the jet-column mode of vortex pairing, occurring at $U_e \cong 30 \text{ ms}^{-1}$, is much more energetic and produces a large $u'_{1/2}$ which essentially equals u'_{ex} at this U_e (this necessitated use of the logarithmic ordinate scale in order to clearly show the amplitude variations).

Similar u'_{ex} and u'_{ux} data, as a function of U_e but for fixed f_p , were obtained for a number of f_p in the 2.54-cm diameter jet. $u'_e/U_e = 1\%$ was used whenever possible; however, since the maximum excitation amplitude available at the jet exit centre-line was not the same for different excitation frequencies (see II), lower excitation levels had to be used at some frequencies which are listed in table 1. It is necessary to document the sensitivity of the turbulence suppression effect to the excitation amplitude before discussing further details of the effect. Values of u'_{ex}/U_e for the 2.54-cm diameter jet, measured at $x/D = 4$ and on the centre-line, are shown in figure 5 as a function of the exit excitation level u'_e/U_e . With $f_p = 1050$ Hz, measurements were made at five different exit speeds within the range where suppression is observed (figure 4); the corresponding St_θ values are indicated in figure 5 for each curve. Figure 5

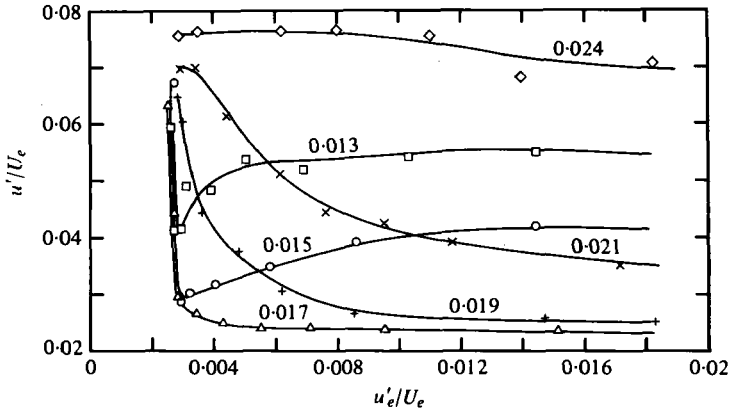


FIGURE 5. Dependence of u' on u'_e for the 2.54 cm circular jet at $f_p = 1050$ Hz, measured on the jet centre-line at $x/D = 4$. Values of St_θ and $Re_D (\times 10^{-3})$ are: \diamond , 0.024, 17.1; \times , 0.021, 18.8; $+$, 0.019, 20.1; \triangle , 0.017, 21.7; \circ , 0.015, 23.6; \square , 0.013, 26.0.

shows that excitation at $St_\theta = 0.017$, which corresponds to $U_e = 12.5 \text{ ms}^{-1}$, produces the minimum u'_{ex} ; the higher St_θ cases correspond to lower exit speeds, and vice versa. The left-most data point for each of the curves in figure 5 represents the corresponding unexcited case. These amplitude responses exhibit a reverse trend about $St_\theta = 0.017$: for St_θ values lower than 0.017, u'_{ex} at first drops substantially but rises with higher u'_e/U_e , while for the higher St_θ values the suppression becomes more pronounced with increasing u'_e/U_e . The increase of u'_{ex}/U_e with increasing u'_e/U_e at the lower St_θ values can be attributed to more regular vortex pairing occurring at higher excitation levels (see I, II).

It is evident that maximum suppression occurs at $St_\theta \cong 0.017$ for all excitation levels, and thus the minimum point in the u'_{ex} curve in figure 4 corresponding to this St_θ (at $U_e = 12.5 \text{ ms}^{-1}$) should remain unaltered even when varying u'_e/U_e is used to obtain the latter data.

It is interesting to view the ratio $u'_{\text{ex}}/u'_{\text{ux}}$ of fluctuation intensities at a point during suppression and without suppression as a measure of the suppression. The suppression factor $u'_{\text{ex}}/u'_{\text{ux}}$ is shown in figure 6(a) as a function of St_D for several excitation frequencies in the 2.54 cm diameter jet. Note that the minimum point representing maximum turbulence suppression shifts systematically to the right with increasing f_p ; the curves at the intermediate frequencies show dual (negative) peaks which were explained during discussion of figure 4. This figure thus confirms our conjecture that St_D does not characterize the condition for maximum suppression. When these data are plotted as a function of the Strouhal number St_θ based on the shear layer momentum thickness at the nozzle exit, as shown in figure 6(b), a reasonably good collapse of the data is evident. Thus, noticeable suppression occurs over the Strouhal number range $0.008 < St_\theta < 0.024$, and the minimum point in each curve falls roughly in the St_θ range of 0.016–0.019.

Similar data for the 12.7 cm and 18 cm circular jets, the plane jet and the single-stream plane mixing layer are shown in figures 7(a), (b), (c) and (d), respectively. Figure 7(e) includes a similar set of data for the plane jet, the excitation in this case being provided by two thin phosphor-bronze ribbons oscillating in the two boundary

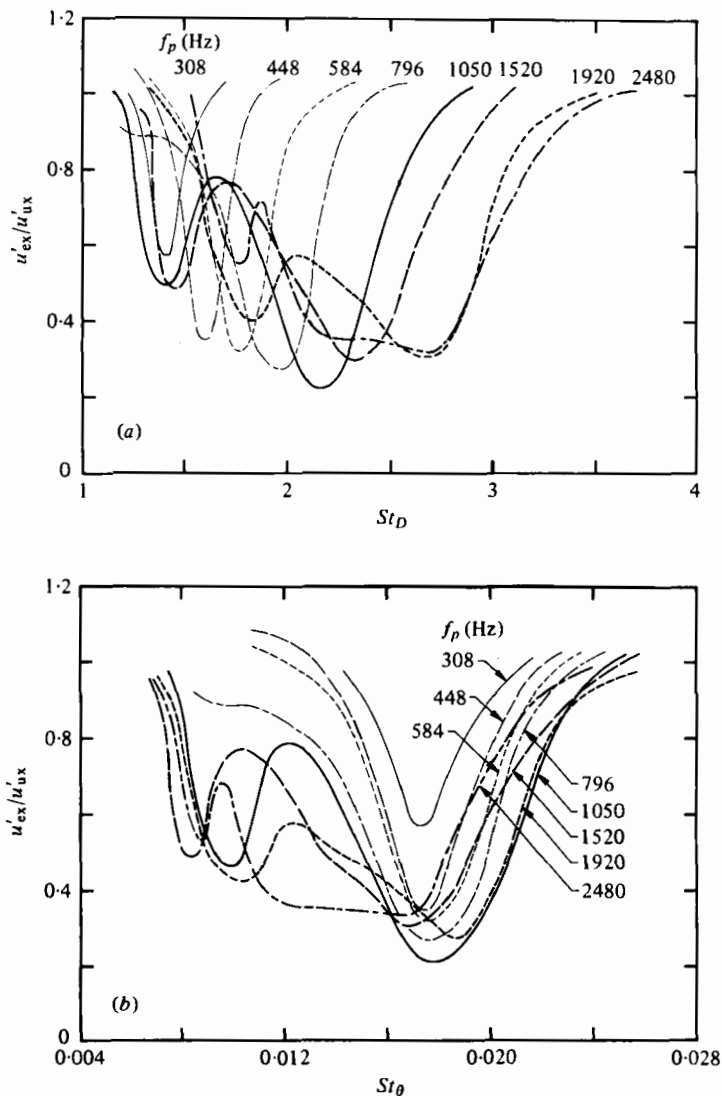


FIGURE 6. (a) Variation of the ratio u'_{ex}/u'_{ux} with St_D for the 2.54 cm circular jet, measured on the jet centre-line at $x/D = 4$; f_p (constant) value for each curve is indicated. (b) u'_{ex}/u'_{ux} data in (a) plotted as functions of St_θ .

layers 4 cm upstream of the lip. Oscillating current in the ribbons, placed in front of electromagnets located outside the flow, makes them oscillate in directions normal to the plane jet nozzle wall (for details see Hussain & Reynolds 1970). The presence of these thin ribbons did not noticeably alter the exit boundary-layer integral characteristics. Data with ribbon oscillation are compared with the corresponding acoustic excitation results. The data in figures 7(a)–(c) and (e) were obtained by keeping f_p constant and varying U_e . The plane mixing layer data in figure 7(d) were obtained by keeping U_e constant and varying f_p . For these latter data, U_e was 10 ms^{-1} , θ_e was 0.0342 cm , and the free-stream velocity fluctuation amplitude u'_f/U_e measured on the exit plane, 1.27 cm from the lip on the high-speed side, was about 0.1% .

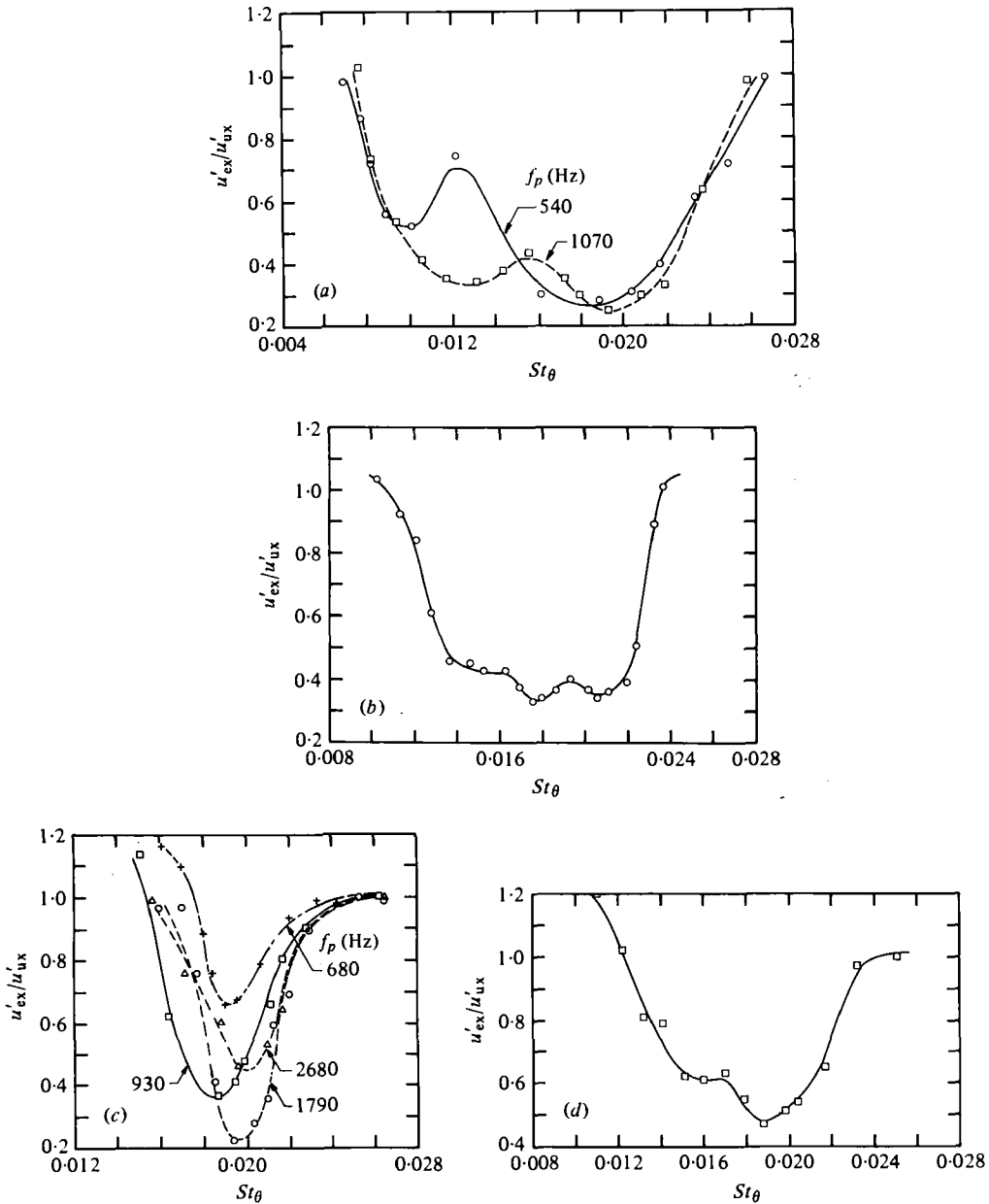


FIGURE 7. Variations of u'_{ex}/u'_{ux} with St_{θ} , measured at $x = 10$ cm and $y = \frac{1}{2}D - 1.27$ cm for the different flows. (a) 12.7 cm circular jet: \circ , $f_p = 540$ Hz; \square , $f_p = 1070$ Hz. (b) 18 cm circular jet, $f_p = 856$ Hz. (c) 3.18 cm plane jet: +, $f_p = 680$ Hz; \square , $f_p = 930$ Hz; \circ , $f_p = 1790$ Hz; \triangle , $f_p = 2680$ Hz. (d) Single-stream plane mixing layer; $U_e = 10$ ms⁻¹. (e) 3.18 cm plane jet, $f_p = 930$ Hz: \square , acoustic excitation; \circ , ribbon excitation.

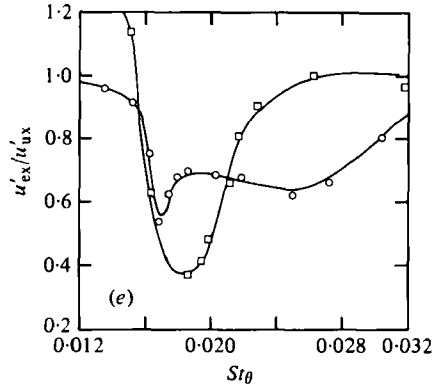


FIGURE 7(e). For legend see p. 143.

For all the data in figures 7(a)–(e), the probe was located at $x = 10$ cm and on the high-speed side at a transverse distance 1.27 cm from the $y = \frac{1}{2}D$ line. Since figure 6(b) clearly indicates that the suppression phenomenon depends on the laminar exit shear layer characteristics† and since the θ_e ranges in which the data were taken in the different flows were approximately the same, the same physical location relative to the nozzle lip was used throughout these experiments.

The u'_{ex}/u'_{ux} data for the two larger circular jets (figures 7a, b) show variations quite similar to those in the 2.54 cm jet, though the St_{θ} range over which the suppression can be observed in the plane jet (figure 7c) is considerably narrower. However, in all the cases in figures 7(a)–(e), maximum turbulence suppression occurs in the neighbourhood of $St_{\theta} = 0.017$.

The ribbon excitation case in figure 7(e) results in suppression over a wider St_{θ} range than the corresponding acoustic excitation. The differences can be due to several factors. Even though the measured mean velocity profile at the exit plane shows no noticeable effect of the presence of the ribbons, slight differences within the data uncertainty may alter the instability characteristics (Crighton & Gaster 1976). There are differences in the nature and level of excitations in the two cases. While acoustic excitation introduces sinusoidal surging almost uniform across the exit plane, the ribbons introduce disturbances in the boundary layers only [Details of the plane jet response to acoustic and ribbon excitations are being investigated in our laboratory.] However, in spite of the inherently different excitations induced acoustically and by ribbons, the fact that both resulted in the turbulence suppression essentially in the same St_{θ} -range illustrates that the suppression phenomenon under study is not associated with acoustic excitation only. At certain conditions of acoustic excitation of jets, an initial reduction in the fluctuation intensities very near to the exit ($x/D \lesssim \frac{1}{4}$) – sometimes referred to as the ‘tail-pipe effect’ – has been observed by many investigators (Crighton 1972; Pfizenmaier 1973; Crighton & Gaster 1976; Hussain & Thomp-

† Limited data in the present experiments showed that the suppression effect did not occur in a jet with turbulent exit boundary layer. Data similar to those in figure 5 taken in the tripped 2.54 cm jet such that the exit boundary layer was fully developed turbulent, at $f_p = 1920$ Hz and in the St_D -range of 1.0 – 3.0 , showed that the ratio u'_{ex}/u'_{ux} was essentially unity. This was checked on the centre-line of the jet for three probe locations, namely, at $x/D = 2, 4,$ and 6 . However, Moore (1977) observed some suppression of noise in tripped jets. A possible suppression effect in jets with turbulent initial conditions remains to be investigated.

son 1980; I and II). As will become clearer with subsequent data in this paper, the turbulence suppression addressed in this paper is not a similar effect but involves suppression of the random velocity fluctuations far downstream from the shear flow origin.

3.2. Shear layer instability and natural roll-up

The spatial stability theory for the growth of a disturbance in a free shear layer (Michalke 1965, 1972) predicts that the maximum *growth rate* should occur at $St_\theta = 0.0165$. By artificial sound excitation of a free shear layer, Freymuth (1966) found maximum growth rate to occur at $St_\theta \cong 0.017$, thereby lending strong support to the theory. It is to be noted that the suppression phenomenon is observed at this same excitation frequency.

The natural roll-up frequency of a free shear layer may be expected to coincide with the maximally unstable mode at $St_\theta \cong 0.017$. That is, given a 'white-noise' type background disturbance, a natural free shear layer is expected to amplify disturbances at $St_\theta \cong 0.017$ the most, and roll up at this same frequency. However, we observe that the roll-up of a free shear layer in the absence of any excitation occurs at a somewhat lower St_θ . This point warrants a detailed discussion here since this forms the basis of our explanation for the observed suppression.

Experimental evidence suggests that a natural free shear layer rolls up at $St_\theta \cong 0.012$. Our study of the free shear layer tone phenomenon (Hussain & Zaman 1978) showed that the shear layer roll-up occurs at $St_\theta \cong 0.012$. Pfizenmaier (1973) also found that the natural roll-up frequency was $St_\theta = 0.0128$ although maximum growth rate in his sound excitation experiments occurred at $St_\theta = 0.017$. Assuming a Blasius profile for the exit boundary layer, one can calculate that the initial roll-up frequencies in Davies & Baxter's (1978) circular-jet experiments corresponded to $St_\theta \cong 0.014$. Similar inferences from Sato's (1959) data in a single free shear layer show that the natural roll-up occurred at $St_\theta \cong 0.012$. From his experiments with Wille, Michalke (1972) cited a mean value of the frequency of initial 'natural disturbances' in a circular nozzle to be $St_{\delta^*} = 0.023$, where δ^* is the exit boundary layer displacement thickness. If a Blasius profile is assumed for the exit boundary layer, this should correspond to $St_\theta \cong 0.009$. Miksad's (1972) experiments in a two-stream free shear layer, however, showed that the natural roll-up coincided with the maximally unstable frequency i.e., it occurred at $St_\theta \cong 0.017$. But in his experiments, a hyperbolic tangent mean velocity profile (on which the spatial stability theory prediction is based) formed only after a significant distance (ten shear-layer thicknesses) from the lip of the splitter plate before which the mean velocity profile was 'wake-like'. Small changes in the shape of the initial profile are known to affect the stability characteristics drastically (Crighton & Gaster 1976). Thus, although the maximally unstable frequency for a free shear layer predicted by the spatial stability theory (at $St_\theta \cong 0.017$, when a disturbance receives maximum amplification rate) has been well-verified by experiments (Freymuth 1966; Miksad 1972; Pfizenmaier 1973), the natural roll-up of the shear layer occurs at a lower St_θ . Preliminary data in a number of free shear flow facilities in our laboratory confirm this observation that the natural roll-up frequency corresponds to $St_\theta \cong 0.012$ (Z. D. Husain, private communication); natural instability of free shear layers is being further investigated in our laboratory.

A plausible clue to the explanation of the above difference could be as follows.

Experimentally, it is observed that for a given shear layer, a disturbance receiving maximum growth rate saturates earlier in x and does not attain large amplitudes. Disturbances at lower frequencies which correspond to larger wavelengths, for this same shear flow, may have lower growth rates but are observed to attain relatively larger amplitudes. Freymuth's (1966) data had shown that although maximum *growth rate* took place at $St_\theta = 0.0176$, the maximum *growth* downstream was achieved at a lower St_θ of about 0.010. It appears that a natural free shear layer rolls up at background disturbance frequencies that are susceptible to a maximum growth rather than maximum growth rate.

Here we would like to draw an analogy with the circular jet 'preferred mode' defined by Crow & Champagne (1971). It was shown by them (also supported by experiments in I, II) that although maximum growth rate of a disturbance in a circular jet occurred at higher Strouhal numbers St_D , maximum growth downstream was attained at $St_D = 0.30$. (Controlled excitation of a plane jet also showed that maximum growth of a disturbance occurs at a lower frequency than that at which the growth rate is the maximum; Hussain & Thompson 1980). Furthermore, Crow & Champagne found through flow visualization that the unexcited circular jet shed vortical 'puffs' at $St_D = 0.30$ rather than at a higher St_D . In other words, when the external excitation frequency matched the natural shedding frequency of the 'puffs', the disturbance received maximum amplification and hence $St_D = 0.30$ was called the 'preferred mode'. In a similar manner, a natural free shear layer appears to lock onto background disturbances that receive maximum amplification downstream rather than to ones receiving maximum initial amplification rate. The mechanism of this selection is not clear to us. Recognizing that the spatial stability theory predictions of Michalke are valid for the linear growth in a parallel flow only, the non-parallel nature inevitable in a practical shear flow and the inherent non-linearities associated with growing disturbances can affect the stability characteristics and thus the natural roll-up process (Ling & Reynolds 1973; Woolley & Karamcheti 1974; Crighton & Gaster 1976; Michalke 1972).

It is necessary to emphasize that the term 'maximum growth' used in this paper refers to the situation where the disturbance is experimentally observed to reach maximum amplitude and 'maximum growth rate' designates the situation where the disturbance faces maximum rate of spatial amplification. Since the flow is non-parallel and is itself in a state of development, even if the shear layer could be regarded as a succession of piecewise parallel flows, neither of these two terms can be regarded as characterizing the eigenmode of the flow at any particular x . Furthermore, as Crighton & Gaster (1976) have shown, the nonparallel flow cannot be regarded as a succession of piecewise parallel flows (Woolley & Karamcheti 1974).

Thus, in a natural free shear layer, we observe that energetic vortices (which are formed with a modal frequency of $St_\theta \cong 0.012$) induce large fluctuation intensities in the near field of the shear layer (inside as well as in the vicinity) both through passage of individual structures and through interactions like pairing. Excitation at $St_\theta \cong 0.017$ forces the disturbance mode at this higher St_θ to grow. Since the growth rate at this St_θ is the largest, but saturation occurs at a much smaller amplitude, the rolled up structures do not grow to sizes as large as in the natural flow. The breakdown of the smaller structures earlier in x and the resulting fine-grained turbulence produces weaker structures and thus weaker 'footprints' outside these structures. As a result,

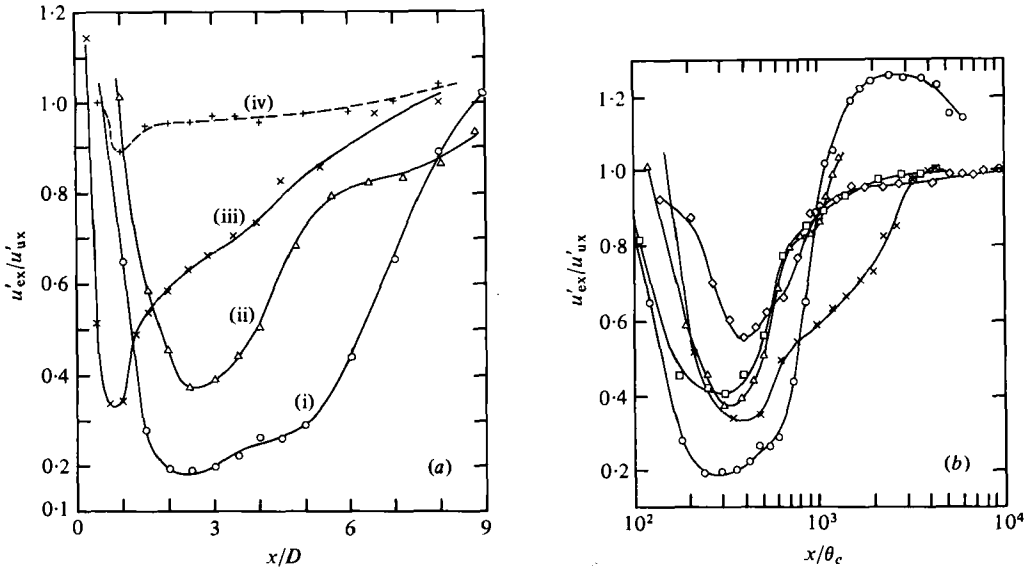


FIGURE 8. Variations of u'_{ex}/u'_{ux} at $St_{\theta} \cong 0.017$: (a) as a function of x/D ; (b) as a function of x/θ_e . The plus symbols in (a) represent data taken along the centre-line of the 18 cm jet; all other data taken along the line $y = \frac{1}{2}D - 1.27$ cm. \times , 18 cm circular jet; \circ , 2.54 cm circular jet; Δ , 3.18 cm plane jet; \square , single-stream plane mixing layer at $U_e = 10$ ms $^{-1}$; \diamond , single-stream plane mixing layer at $U_e = 20$ ms $^{-1}$.

Flow	f_p (Hz)	u'_e/U_e	Re_D	θ_e (cm)	Re_{θ}	St_{θ}
2.54 cm circular jet	1050	1 %	2.1×10^4	0.0208	172	0.017
3.18 cm plane jet	1720	0.3 %	4.9×10^4	0.0249	385	0.018
18 cm circular jet	856	0.3 %	20×10^4	0.0363	408	0.018
90 cm wide plane mixing layer	600	—	—	0.0354	269	0.018
	1680	—	—	0.0205	269	0.017

TABLE 2. Excitation conditions.

lower fluctuation intensities are encountered everywhere. (The coherent structures in the natural and the excitation cases will be discussed later.) In the case of a circular jet, the formation of the natural structure in the near field is more complex because of the 'jet preferred mode' (occurring at $St_D = 0.30$, independent of the exit shear layer characteristics; see Crow & Champagne 1971; II). While the exit shear layer, if laminar, is still expected to roll up at $St_{\theta} \cong 0.012$, the preferred structure at $St_D = 0.30$ may be achieved through a number of stages of pairing (Browand & Laufer 1975) and very large fluctuation intensities can be encountered in the jet core.

3.3. The spatial extent of suppression

Figure 3 showed that the suppression effect could be noticed up to about $x/D = 8$. But since the phenomenon is dependent upon the jet exit boundary layer characteristics, it was conjectured that this axial range, as well as the transverse distance at a particular x over which the suppression occurs, would scale on the initial shear layer

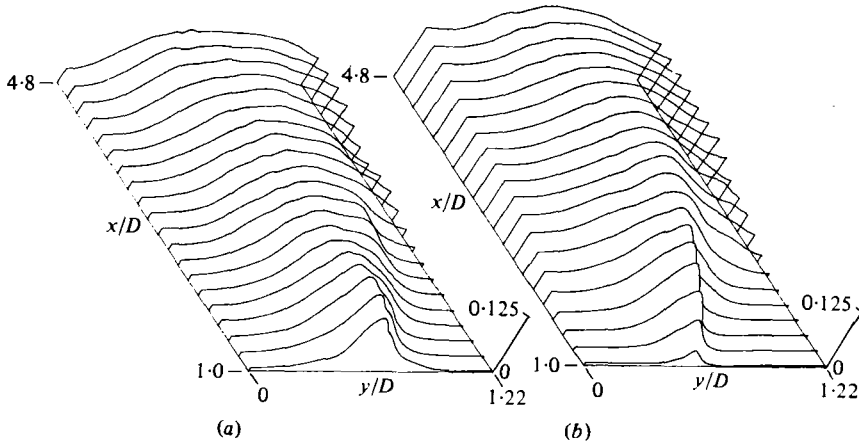


FIGURE 9. Distributions of $u'(x, y)/U_e$ in the 2.54 cm circular jet at $Re_D = 2.14 \times 10^4$: (a) excited at $St_\theta = 0.017$ ($St_D = 2.15$); (b) unexcited.

characteristic width and, therefore, vary from nozzle to nozzle and with Re_D . The x extent of the suppression effect was therefore investigated in the different flows under study.

The axial variation of the suppression factor u'_{ex}/u'_{ux} in the three jets for excitation at $St_\theta \approx 0.017$ are shown in figure 8(a). Curves (i) and (iv) are for the centre-line of the 2.54 cm and the 18 cm jets, respectively. As curve (iv) shows, the centre-line in the 18 cm jet being far from the shear layer, the suppression effect can hardly be noticed on the centre-line. But if the probe is brought closer to the shear layer, e.g. at $y = D/2 - 1.27$ cm, suppression is observed over the distance $0.5 \lesssim x/D \lesssim 8$, as shown by curve (iii). The initial momentum thicknesses and the excitation conditions for the three flows in figure 8(a) are listed in table 2. Curves (i), (ii) and (iii), for the three largely different jets, show similar trends in the u'_{ex}/u'_{ux} variation with x . The ratio u'_{ex}/u'_{ux} reaches small values shortly after the exit, and the location and extent of the minimum point varies from jet to jet, but in all the three cases it rises to a value of unity at around $x/D = 8$.

The same data as shown in figure 8(a) are replotted in figure 8(b) (except for the centre-line data in the 18 cm jet) as a function of x/θ_e , together with two sets of similar data in the plane mixing layer. Note that the abscissa in figure 8(b) is logarithmic in order to accommodate the large extent of the downstream distances over which the suppression effect is observed. The values of θ_e and the excitation parameters for the mixing layer cases are also listed in table 2. Consistent with the other data, the x traverse for the plane mixing layer case was done also along a line parallel to the x axis but 1.27 cm from the lip on the high-speed side. These data show that the maximum turbulence suppression occurs at a distance $300\theta_e \lesssim x \lesssim 500\theta_e$. Note that farther downstream in the 2.54 cm jet (for $x/\theta_e \approx 1100$, corresponding to $x/D \approx 9$), u'_{ex}/u'_{ux} is actually higher than unity (see also figure 3). This trend of u'_{ex}/u'_{ux} reaching values higher than 1 was also observed with the plane jet, but not with the larger circular jet (18 cm) or the plane mixing layer. The rightmost data point for the 2.54 cm jet in figure 8(b) corresponds to $x/D = 50$. Note that for the plane mixing layer, the suppression could be detected as far downstream as $x = 6000\theta_e$.

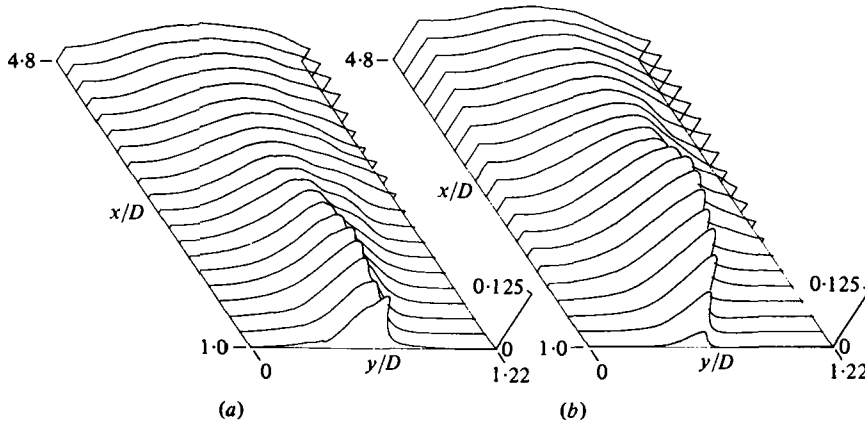


FIGURE 10. Distributions of $v'(x, y)/U_0$ corresponding to the flow in figure 9: (a) excited; (b) unexcited.

It appears that the axial extent over which the suppression effect can be observed in a jet is determined by the diameter of the jet (or the width of the plane jet). The centre-line turbulence intensity in a jet (circular or plane; excited or unexcited) reaches a peak at $x/D \cong 8$. This peak has been observed to shift upstream under excitation conditions when there are large initial amplifications of the disturbance, e.g. at $St_D = 0.30$ or 0.85 (Crow & Champagne 1971; Hussain & Thompson 1980; Hasan & Hussain 1980; I; II); or, as figure 3 shows, the peak of the centre-line longitudinal fluctuation intensity at $x/D \cong 8$ can move downstream when suppression is observed. Even though the location of this peak shifts slightly upstream or downstream, its amplitude is not significantly affected by excitation (see I). This peak is believed to be associated with the interactions of the large-scale coherent structures at the end of the potential core; in case of the plane jet, this is the region of interaction of the two shear layers. Excitation at $St_\theta \cong 0.017$ eliminates the formation of energetic large-scale structures, otherwise occurring farther downstream at $St_\theta \cong 0.012$, and this manifests itself in a lengthening of the core (the length before direct interaction between the opposite mixing layers commences). Presumably, these interactions at $x/D \cong 8$ are not affected noticeably by excitation because the shear layer structure becomes progressively oblivious of the initial structure and thus the observed suppression effect in a jet is essentially terminated at $x/D \cong 8$ by the large turbulence intensities generated by these interactions. This is the reason why the effect of excitation at $x/D \lesssim 8$ in the 18 cm jet is quite different from those for the smaller circular and plane jets, because the dimensional distance from the lip to $x/D \cong 8$ is considerably larger for the 18 cm jet; that is, the shear layer structure may have recovered from the effect of the excitation at this large streamwise distance. Since in a plane mixing layer there is no such interaction from another layer terminating the initial evolution, the suppression effect is expected to persist for a longer distance and is indeed observed to do so in figure 8(b).

3.4. The flow-field details of suppression for a typical case

In an effort to better understand the mechanism of turbulence intensity suppression, a specific case of excitation at $St_\theta = 0.017$ was studied in greater detail. Unless other-

wise stated, the following discussion refers to the 2.54 cm diameter jet at $Re_D = 21\,000$, excited at $f_p = 1050$ Hz with $u'_e/U_e = 1\%$.

It was desirable to first check whether the suppression occurred only in the jet potential core or over the entire width of the jet including the shear layer. The distribution of the longitudinal and transverse components of the turbulence intensities u' , v' and the time-averaged Reynolds stress $\overline{u'v'}$ were measured over a diametral plane. The u'/U_e distributions for the region $1 \leq x/D \leq 4.8$ and $0 \leq y/D \leq 1.22$ are shown as relief maps in figure 9(a) for the excited case and in figure 9(b) for the corresponding unexcited case. It is clear that for the excitation case the turbulence intensity is lower over the entire cross-section of the jet, as compared to the corresponding values in the unexcited case. The distributions of v'/U_e , similarly presented as relief maps in figures 10(a) and (b) for the excited and the unexcited cases, respectively, show a similar suppression in the transverse component of the turbulence intensity also. Note that for a particular y , the suppression (i.e. when $u'_{ex} < u'_{ux}$) is observed after a particular longitudinal distance (x) which is different for different y ; for example, $u'_{ex} < u'_{ux}$ occurs for $x/D > 0.75$ on the centre-line while in the shear layer it occurs for $x/D > 1.4$. Nearer to the jet exit (within $0 < x/D < 1$), the peak values of u' and v' in the middle of the shear layer are larger for the excited case because of the rapid growth in x of the mode of maximum growth rate before the growth is arrested due to saturation and turbulent breakdown, as explained earlier. (Values of u' and v' were measured in the range $0 < x/D < 1$ but are not shown partly because of the poor spatial resolution with the x -wire probe in the thin shear layer and partly because these time average data near the lip are not of further help in understanding the suppression mechanism any better.)

The Reynolds stress, $\overline{u'v'}/U_e^2$, distributions in the x - y range corresponding to figures 9 and 10 are shown in figures 11(a) and (b) for the excited and the unexcited cases, respectively. The peak Reynolds stress encountered in the shear layer for the excitation case becomes less than the corresponding values in the unexcited case for $x/D > 1.4$. The substantially lower values of $\overline{u'v'}$ farther downstream for the excitation case suggests that the flow there does not involve strong large-scale vortical interactions like pairing (see Hussain & Zaman 1980). There is indication of one stage of pairing (see spectra, pictures and educed structures discussed later) for the excitation case at an upstream location $x/D \cong 1$, where $\overline{u'v'}$ values are indeed higher in the excited case than in the unexcited. Flow-visualization and conditionally sampled data (see later) substantiate the perceptions of the effect of excitation on the structures as discussed above.

The spectra of the \tilde{u} -signal at different x -stations on the jet centre-line are shown in figure 12. For each x station (indicated on the right-hand side) two spectrum traces are shown – the solid line representing the excitation case and the dotted line the corresponding unexcited case; the vertical (logarithmic) and the horizontal (linear) scales are the same for all the traces. The vertical bar on the right-hand side for each trace represents the total r.m.s. value of the u -fluctuations. For the excitation case, the spectral spike at the excitation frequency ($f_p = 1050$ Hz) diminishes rapidly and cannot be discerned beyond $x = 3D$. At $x/D = 1.5$, there appears a small spike at the subharmonic frequency (525 Hz) which grows somewhat and persists in the spectra up to $x/D = 4$ indicating the (intermittent) occurrence of one stage of vortex pairing. For the unexcited case on the other hand (the dotted traces), a large broadband

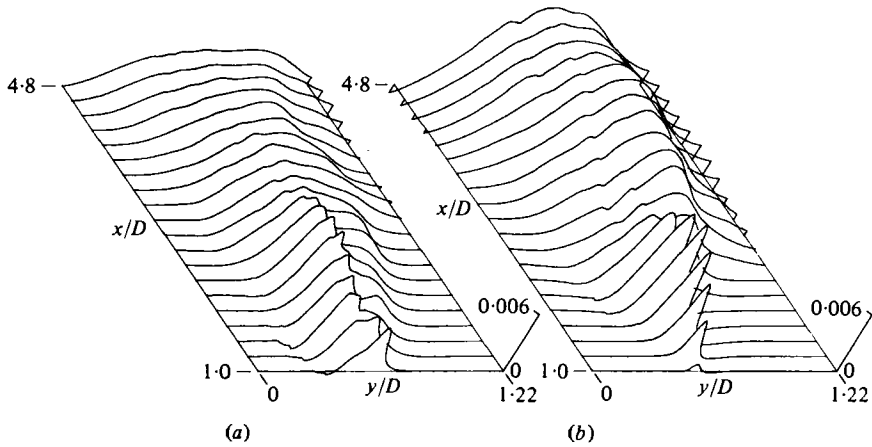


FIGURE 11. Distributions of $\overline{uv}(x, y)/U_a^2$ corresponding to the flow in figure 9: (a) excited; (b) unexcited.

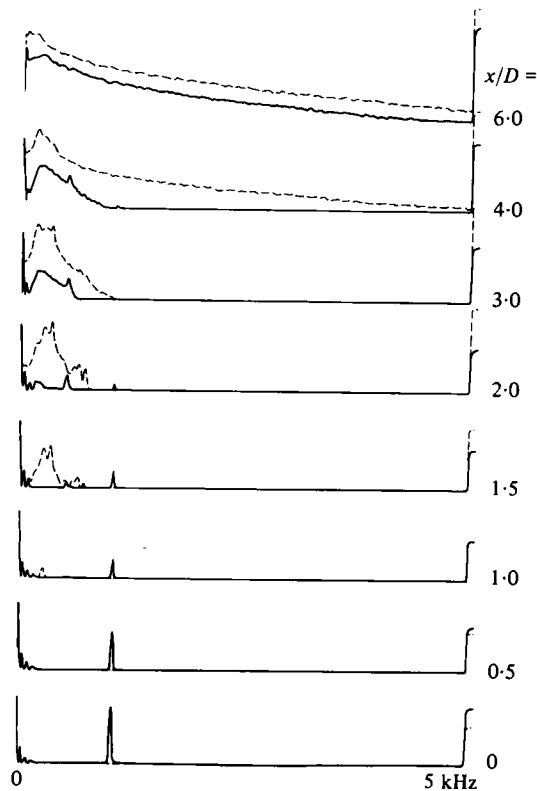


FIGURE 12. \tilde{u} -spectra at different x on the centre-line of the 2.54 cm jet for $U_a = 12.7 \text{ ms}^{-1}$ ($Re_D = 2.14 \times 10^4$); solid lines represent the excitation case at $St_\theta = 0.017$, dashed lines represent the corresponding unexcited flow; each pair of traces have same co-ordinate origin. Identical vertical (logarithmic) and horizontal (linear) scales used for all traces.

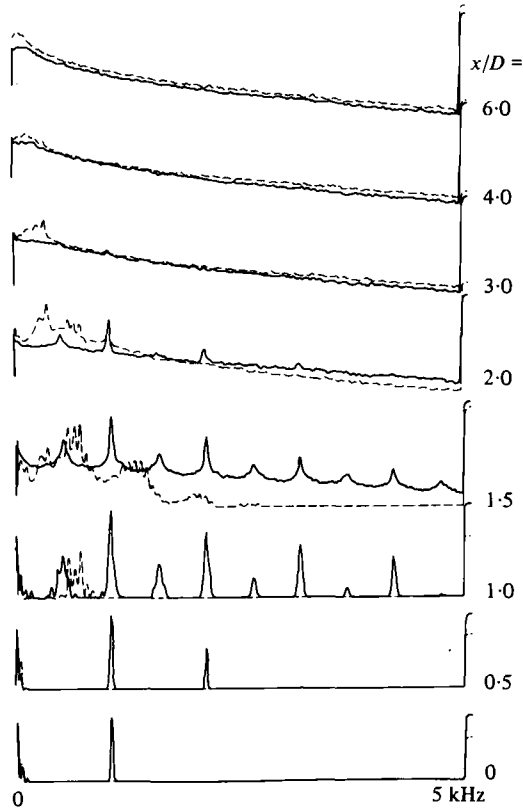


FIGURE 13. \bar{u} -spectra at different x along a line where $U/U_e = 0.90$. Other details are the same as in figure 12.

spectral peak appears (around $f = 360$ Hz) at $x/D = 1.5$. The effect of excitation at $St_\theta = 0.017$ ($f_p = 1050$ Hz) is to suppress this broadband peak and as a result, u' for the excitation case is much lower. For $x/D \gtrsim 4$, the spectra show that the suppression of the turbulent kinetic energy occurs over the entire frequency range. This is not unexpected because energy at higher frequencies for the unexcited case should depend on the strength of the upstream modes (say, the peak at $f \approx 360$ Hz) from which the spectrum evolves through nonlinear broadening; since excitation reduces this low-frequency peak, the energy cascade to higher frequencies is also retarded.

Spectra at different x -stations, measured at transverse locations where $U/U_e = 0.90$, are shown in figure 13, in a fashion similar to figure 12. At each x , the transverse probe location was chosen to be the $U/U_e = 0.9$ point in the mean velocity profile of the unexcited flow, and both the spectrum traces for the excited and unexcited flows were obtained with the probe location unchanged. It should be emphasized that the transverse shift of the physical location of the $U/U_e = 0.9$ point of the profile between the excited and the unexcited cases was found to be small compared to the mixing layer width. Ideally, for such comparison, spectra for the excited and unexcited cases should be obtained at the same relative transverse location with respect to the shear layer boundary. However, since the spectrum is not sensitive to small variations in the transverse location near the boundary of the mixing layer, comparison of the two

spectra presented is still valid. Note that in both figures 12 and 13, the spectrum traces for the unexcited flow at the jet exit (hidden behind the solid lines) do not show any conspicuous spectral content except at the very low frequencies.

For the excitation case, the spike at $f_p = 1050$ Hz (figure 13) grows up to $x/D \cong 1.5$ before starting to decay. Spectral peaks at higher harmonics (of f_p) as well as the first subharmonic ($\frac{1}{2}f_p$) and its harmonics are prominent at $x/D = 1$, representing passage of strongly organized vortices. The higher harmonic peaks are merely due to distortions of the signal and as far as the large-scale motions are concerned, only the peaks at $\frac{1}{2}f_p$ and f_p are of significance (see II). The peak at the subharmonic frequency at any location indicates a completed or an ongoing stage of vortex pairing. Thus, while for the excitation case only one stage of pairing can be discerned, the unexcited case indicates two stages of pairing within the downstream distance of $x/D \cong 4$. For the latter case, at $x/D = 1$, there is a large peak at $f = 720$ Hz, which represents the roll-up frequency of the vortices (corresponding to $St_\theta = 0.012$). Note that the centre-line being far away from the shear layer, this peak is not visible in the spectra at the same x station in figure 12. A peak at the subharmonic frequency (i.e., at 360 Hz) appears at $x/D = 1.5$ and keeps growing farther downstream while the peak at 720 Hz diminishes. In both the figures 12 and 13 for $x/D \cong 4$, maximum energy for the unexcited case occurs at the second subharmonic of 720 Hz (i.e., at 180 Hz) which corresponds to $St_D \cong 0.35$. This is the 'terminal Strouhal number' at this Re_D for this jet (Browand & Laufer 1975), and is reached after two stages of vortex pairing.

3.5. The large-scale coherent structures in the flow with and without excitation

(a) *Flow visualization*: In an attempt to extend our understanding of the suppression phenomenon, the excitation-induced modification of the large-scale coherent structures was explored through flow-visualization. While it is not possible to photographically capture the kinematic details of our observations, a few sample pictures will be included to support the claims. The pictures were obtained by introducing one streak of smoke from inside the settling chamber and by illumination with a high intensity stroboscope. The camera shutter speed was set such that one stroboscopic flash (of duration 2–3 μ s) occurred during the time the shutter was open. Each picture thus provides an instantaneous pattern of the smoke concentration in the shear layer. Several pictures for each of the two cases were obtained, and the ones shown are representatives of the two sets. The effect of turbulence suppression is captured in pictures shown as figures 14(a) and (b). While the picture for the unexcited case in (a) clearly shows the roll-up occurring at around $x/D = 1.25$, large-scale coherent vortical motions are not apparent in (b) for the excitation case. Farther downstream, the picture for the unexcited case shows undulations on the high-speed side, indicating large-scale coherent motions; but the excited flow indicates a relatively undisturbed motion in the potential core and fine-grained turbulence in the shear layer.

The spectrum traces in figure 13, for the excitation case at $x/D = 1.5$, show clear spikes at the fundamental driving frequency and its subharmonic. Thus, coherent structures involving one stage of pairing were expected to be visible in figure 14(b); for this case $f_p = 1050$ Hz. Visual observation with stroboscopic illumination occasionally indicated roll-up of very small vortices at small spacings. Shortly afterwards, one stage of pairing of these vortices was also observed but the illumination and

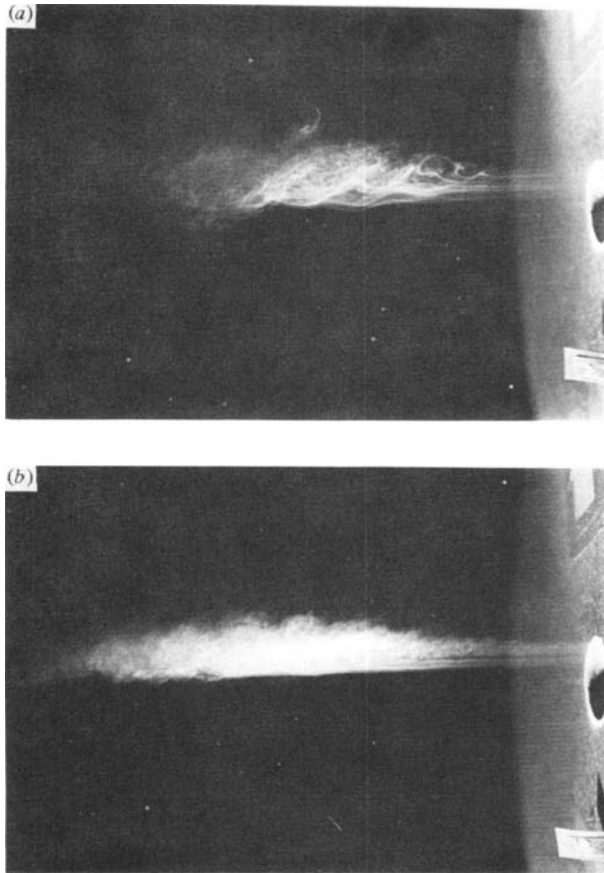


FIGURE 14. The 2.54 cm jet flow at $U_e = 12.7 \text{ ms}^{-1}$ ($Re_D = 2.14 \times 10^4$):
 (a) unexcited; (b) excited at $St_\theta = 0.017$ ($St_D = 2.15$).

photographic technique, in this high-speed flow with the small vortices, failed to capture the details. However, lack of strong coherent motions in the shear layer downstream is quite evident. Furthermore, on careful scrutiny, a lengthening of the potential core in the excitation case should be apparent.

The visualization technique, however, was successful in clearly capturing shear layer structures with and without excitation at a lower speed. Pictures taken in the 7.62 cm jet are shown in figure 15: for the unexcited flow in (a) and for excitation at $St_\theta = 0.017$ in (b); the exit velocity U_e for both cases was 6.1 ms^{-1} ($\theta_e = 0.029 \text{ cm}$). At $x = 10 \text{ cm}$ and $y = \frac{1}{2}D - 1.27 \text{ cm}$, u'_{ex}/u'_{ux} was found to be about 0.50. Close-up views of the flow field extending over $0 < x \lesssim 8 \text{ cm}$ are shown in these pictures, and large-scale vortical structures are visible in both. For the $St_\theta = 0.017$ case, figure 15(b) clearly shows one stage of pairing, an earlier transition to fine-grained turbulence, and somewhat elongated vortical structures with diffuse cores following the pairing stage. The smoke spiral in figure 15(a) for the unexcited case, on the other hand, indicates more energetic vortical structures persisting farther downstream in the flow. Thus, the observed suppression of the large-intensity fluctuations by excitation is achieved by inhibiting the formation of the strong and energetic vortical structures otherwise found in the unexcited shear layer.

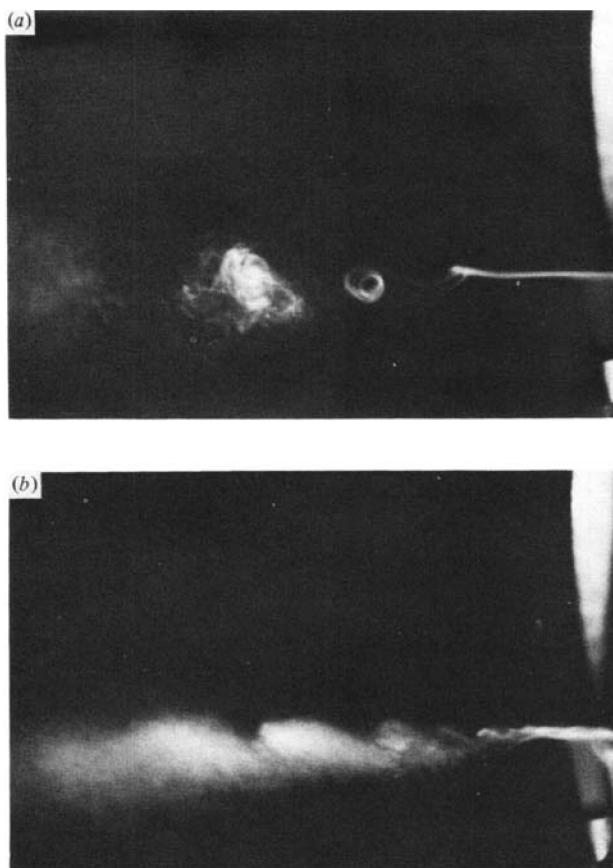


FIGURE 15. The 7.62 cm jet flow at $U_e = 6.1 \text{ ms}^{-1}$ ($Re_D = 3.2 \times 10^4$):
 (a) unexcited; (b) excited at $St_\theta = 0.017$ ($St_D = 5.5$).

(b) *Educed coherent structures*: Conditional measurements were carried out to reduce the most dominant large-scale structures in the excited and unexcited flows; measurements were made at $x/D = 1.5$ in the 2.54 cm jet. A reference (single wire) hot-wire probe was placed on the jet centre-line at $x/D = 1.5$, while an X-wire probe was traversed in y at the same x station, and the instantaneous \tilde{u} signals were obtained from the X-wire signals by an analog turbulence processor. For the unexcited case (for which the dominant roll-up frequency is 720 Hz), the reference signal was band-pass filtered between 300–400 Hz; and for the excited case ($f_p = 1050$ Hz), between 500–600 Hz. The filtered reference probe signal in either case thus captured the oscillation at the subharmonic of the initial roll-up frequency. At each y station, time series data of the filtered reference signal and the $\tilde{u}(t)$ and $\tilde{v}(t)$ signals were recorded simultaneously on a magnetic tape at a sampling frequency of 8 kHz for each.

Sample plots of the reference signal showed that the periodicities with large amplitudes at the subharmonic frequencies (i.e., about 360 Hz for the natural case and 525 Hz for the excitation case) occurred occasionally. For each of the cases, a threshold level for the reference signal was chosen (with positive value and positive slope) to sample the data. For the different y stations, ensemble averages u_p and v_p (of \tilde{u} and \tilde{v}) were computed from sample functions beginning from the instants every time the

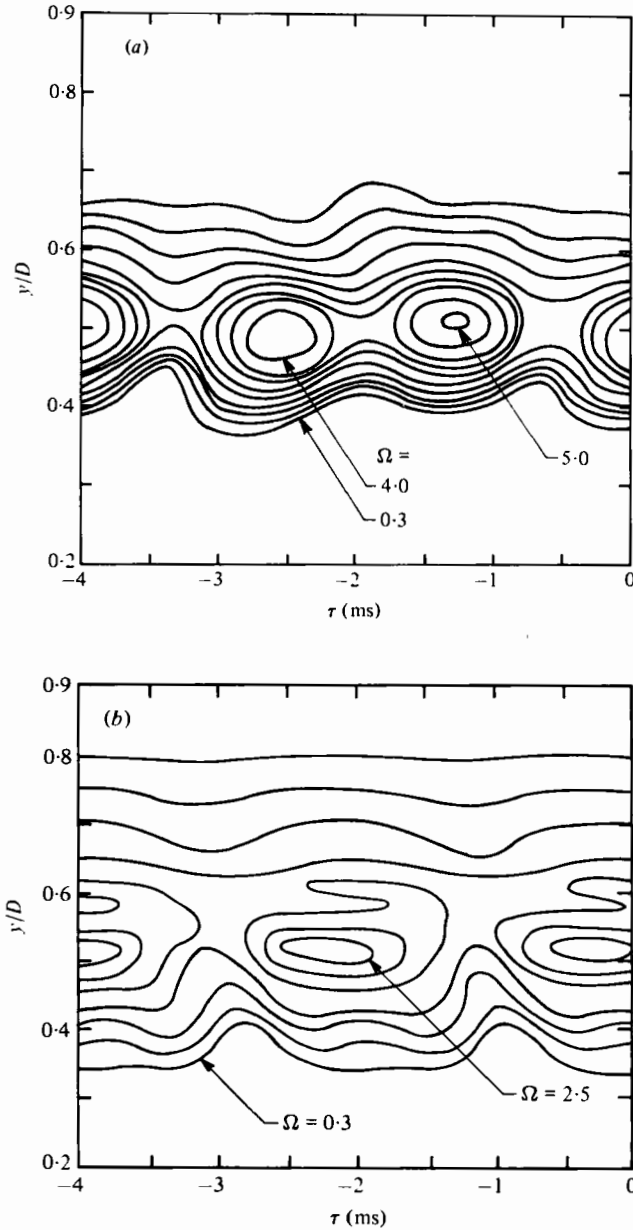


FIGURE 16. Distribution of azimuthal vorticity Ω for the 2.54 cm circular jet, educed at $x/D = 1.5$; $Re_D = 2.14 \times 10^4$: (a), unexcited flow; (b), excitation at $St_\theta = 0.017$. Ω is non-dimensionalized by the excitation frequency f_p ($= 1050$ Hz). Contour levels in sequence are 0.3, 0.5, 0.7, 1.0, 1.5, 2.0, 2.5, 3.0, 4.0 and 5.0.

chosen threshold was exceeded. Thus, the distributions of ensemble average velocities u_p and v_p were obtained on a (t, y) plane. By least squares-fit of a third order polynomial over five adjacent data points (Zaman 1978), the distributions of $\partial u_p / \partial y$ and $\partial v_p / \partial t$ were then obtained. Using the Taylor hypothesis, the z component of the vorticity Ω ($= -(\frac{1}{2}U_e)^{-1} \partial v_p / \partial t - \partial u_p / \partial y$) was thus computed as a function of t and y .

The choice of the threshold level for data sampling in each of the two cases was clearly arbitrary. However, for the threshold condition chosen, the accepted data records represented about 8% of the total time series recorded for each of the unexcited and the excited flows. Several trial computations for the vorticity showed that a much lower threshold level smeared the computed vorticity contours while a much higher threshold resulted in large uncertainties in the $\Omega(t, y)$ data (because of reduced ensemble size). However, small variations about the accepted thresholds did not noticeably alter the vorticity distributions.

The vorticity contours are shown in figures 16(a) and (b) for the unexcited and the excited cases, respectively. The large-scale vortical structures at $x/D = 1.5$, for the excitation case at $f_p = 1050$ Hz, are clearly captured in figure 16(b). The vortices here are after one stage of pairing. Note that the spacing of the vortices is about 1.9 ms corresponding to the subharmonic frequency of 525 Hz. The vortical structures captured in figure 16(a) for the unexcited jet, on the other hand, are spaced at about 1.4 ms corresponding to the initial roll-up frequency of 720 Hz ($St_\theta = 0.012$). But alternate vortices are slightly staggered indicating the impending first pairing stage and explaining the subharmonic peak in the spectrum (figure 13).

A question naturally arises as to what extent the smoke traces continue to mark the boundaries of the vortical structures. For a laminar free shear flow, the vorticity contours are expected to bear close resemblance with the streakline patterns (Michalke 1972). As the rolled up vortices containing the injected smoke streaks start breaking down, the smoke should fill the entire cores of the vortical structures. Since the molecular diffusion time scale is many times the flow or turbulence time scale, the smoke boundaries cannot be significantly different from the structure boundaries, for the downstream distances over which the smoke traces are visible in figures 14 and 15. Careful examination reveals similarity between the smoke pictures in figures 14(a) and 15(a) with the vorticity contours in figure 16(a). Some resemblance can also be observed between the smoke picture in figure 15(b) with the contours in figure 16(b), both for the excitation case.

The measured peak vorticity in the cores in figure 16(a) is about twice that in figure 16(b). Thus, the vortices found in the unexcited jet, at least at the measurement station, are much stronger than those in the excitation case. In the latter case, the vorticity has also diffused over a wider transverse distance. Note that the relative sizes of the structures in the two cases are also consistent. Even though the rolled up vortices under excitation at $St_\theta \cong 0.017$ are smaller, the structure captured at $x/D = 1.5$ in figure 16(b) is larger because each is the result of merger of two smaller vortices. For the unexcited case, the reduced structure is still the initially rolled-up vortex slightly prior to the first pairing. These data appear to qualitatively agree with the visualization pictures and substantially confirm our inference based on examinations of the hot-wire signals that the relatively strong vortices with high core vorticity, found in a natural shear layer, are inhibited from being formed when excited at $St_\theta \cong 0.017$. The fluctuation intensities, encountered in the natural shear layer owing to the passage of these vortices, are thus suppressed by the inhibition of the formation of these energetic vortices.

4. Concluding remarks

The phenomenon of turbulence suppression in the near field of a free shear flow under controlled excitation has been explored through experimental investigations in four circular jets, a plane jet, and a plane mixing layer. The suppression effect in all these flows has been documented and the excitation conditions producing maximum suppression have been identified. It has been shown that the suppression is a consequence of excitation-induced modification of the shear layer structure, and occurs at the excitation frequency corresponding to the 'maximally unstable' disturbance frequency of the initial free shear layer. The phenomenon is thus found to be associated with the shear layer instability and occurs not only in circular jets, but also in plane jets and mixing layers.

It is observed that a free shear layer naturally rolls up at a frequency different from the 'maximally unstable' frequency. The suppression effect occurs when the shear layer is excited at frequencies above the natural roll-up frequency f_n ; the most pronounced suppression occurs at a frequency f_s which is about 40 % higher than f_n . The spatial stability theory, well-verified by experiments, predicts a frequency f_m at which a disturbance experiences the maximum growth rate. Our data, in the variety of the flows studied, show that $f_s \cong f_m$, the corresponding Strouhal number $St_\theta (\equiv f_s \theta_e / U_e)$ being about 0.017.

The suppression effect (under excitation at $St_\theta \cong 0.017$) occurs over the entire width as well as in the vicinity of a shear layer. The axial extent over which it is observed in a jet is determined by the jet diameter (or width of a plane jet) and is found to be $0.75 < x/D \lesssim 8$. For the smaller jets, the effect of suppression is to lengthen the potential core and shift the virtual origin downstream by about 3–4 diameters. For the single-stream plane mixing layer, the suppression could be detected as far downstream as $x = 6000\theta_e$.

For a typical case of turbulence suppression under excitation and the corresponding unexcited flow, the flow-field details are documented. Spectral analysis of the velocity signal reveals that the reduction of turbulent kinetic energy under excitation occurs over the entire frequency range. For the unexcited flow, a broadband peak with a modal frequency corresponding to $St_\theta \cong 0.012$ appears in the spectra at $x/D \cong 1.5$. This is followed by the generation of large-amplitude subharmonic peaks, indicating two stages of vortex pairing within a distance of $x/D \cong 4$. Excitation removes these peaks from the spectra; the spectral spike at the fundamental (driving frequency) grows rapidly, saturates and breaks down within a short distance downstream. Generation of a subharmonic peak at around $x/D = 1$ indicates the occurrence of one stage of pairing in the excitation case, but neither of the peaks at f_p and $\frac{1}{2}f_p$ reaches an amplitude as large as those in the unexcited flow.

Flow-visualization shows the presence of strong, large-scale vortical structures in the unexcited flow. Under excitation at $St_\theta \cong 0.017$, the shear layer rolls up in closely packed, smaller vortices and undergoes breakdown into fine-grained turbulence following one stage of pairing. Farther downstream, the large-scale structures are visible but have diffuse cores. As a consequence, the fluctuation intensity both inside and outside the shear layer is noticeably weaker than the corresponding unexcited case. These observations are consistent with the strengths and sizes of structures deduced in the two flows by conditional sampling measurements. It is concluded that

excitation at $St_\theta \cong 0.017$ produces rapid roll-up and early breakdown of the shear layer and thus inhibits the formation of the energetic large-scale vortices which otherwise survive farther downstream, grow to larger sizes, and undergo successive pairings in the corresponding unexcited flow. The consequence is that the large fluctuation intensities, otherwise caused by the passage and interaction of those energetic vortices, are reduced everywhere in the presence of excitation at $St_\theta \cong 0.017$.

The authors are grateful to Professor G. H. Koopmann for a careful review of the manuscript. This research was supported by NASA Langley Research Center Grant NSG-1475 and Office of Naval Research Grant N00014-76-C-0128.

REFERENCES

- BECKER, H. A. & MASSARO, T. A. 1968 *J. Fluid Mech.* **31**, 435.
- BROWAND, F. K. & LAUFER, J. 1975 *Turb. in Liquids*, **5**, 333. University of Missouri-Rolla.
- BROWN, G. B. 1935 *Proc. Phys. Soc.* **47**, 703.
- CHAN, Y. Y. 1974 *Phys. Fluids* **17**, 1667.
- CHANAUD, R. C. & POWELL, A. 1965 *J. Acous. Soc. Am.* **37**, 902.
- CLARK, A. R. 1979 Ph.D. dissertation, University of Houston.
- CRIGHTON, D. G. 1972 *J. Fluid Mech.* **56**, 683.
- CRIGHTON, D. G. & GASTER, M. 1976 *J. Fluid Mech.* **77**, 397.
- CROW, S. C. & CHAMPAGNE, F. H. 1971 *J. Fluid Mech.* **48**, 547.
- DAVIES, P. O. A. L. & BAXTER, D. R. J. 1978 *Structure and Mechanisms of Turbulence I*, Lecture Notes in Physics, vol. 75 (ed. H. Fiedler), p. 125. Springer.
- FREYMUTH, P. 1966 *J. Fluid Mech.* **25**, 683.
- HASAN, M. A. Z. & HUSSAIN, A. K. M. F. 1980 *J. Fluid Mech.* (submitted).
- HUSSAIN, Z. D. & HUSSAIN, A. K. M. F. 1979 *A.I.A.A. J.* **17**, 48.
- HUSSAIN, A. K. M. F. & CLARK, A. R. 1977 *Phys. Fluids* **20**, 1416.
- HUSSAIN, A. K. M. F. & REYNOLDS, W. C. 1970 *J. Fluid Mech.* **41**, 241.
- HUSSAIN, A. K. M. F. & THOMPSON, C. A. 1980 *J. Fluid Mech.* **100**, 397.
- HUSSAIN, A. K. M. F. & ZAMAN, K. B. M. Q. 1975 *Proc. 3rd Interagency Symp. on Univ. Res. in Transportation Noise, Univ. of Utah*, p. 314.
- HUSSAIN, A. K. M. F. & ZAMAN, K. B. M. Q. 1978 *J. Fluid Mech.* **87**, 349.
- HUSSAIN, A. K. M. F. & ZAMAN, K. B. M. Q. 1980 *J. Fluid Mech.* **101**, 493.
- KIBENS, V. 1979 *A.I.A.A. Paper* no. 79-0592.
- LING, C. & REYNOLDS, W. C. 1973 *J. Fluid Mech.* **59**, 571.
- MICHALKE, A. 1965 *J. Fluid Mech.* **22**, 351.
- MICHALKE, A. 1972 *Prog. Aero. Sci.* **12**, 213.
- MIKSAD, R. W. 1972 *J. Fluid Mech.* **56**, 695.
- MOORE, C. J. 1977 *J. Fluid Mech.* **80**, 321.
- PETERSEN, R. A., KAPLAN, R. E. & LAUFER, J. 1974 *N.A.S.A. Contractor Rep.* no. 134733.
- PFIZENMAIER, E. 1973 Doktor-Ingenieur Thesis, Technische Universität Berlin.
- ROCKWELL, D. O. 1972 *Trans. A.S.M.E. E, J. Appl. Mech.* **39**, 883.
- SATO, H. 1959 *J. Phys. Soc. Japan* **14**, 1797.
- SATO, H. 1960 *J. Fluid Mech.* **7**, 53.
- VLASOV, Y. V. & GINEVSKIY, A. S. 1974 *N.A.S.A. TT F-15*, 721.
- WILLE, R. 1963 *Z. Flugwiss.* **11**, 222.
- WOOLLEY, J. P. & KARAMCHETI, J. 1974 *A.I.A.A. J.* **12**, 1457.
- ZAMAN, K. B. M. Q. 1978 Ph.D. dissertation, University of Houston.
- ZAMAN, K. B. M. Q. & HUSSAIN, A. K. M. F. 1977 *Proc. Symp. Turbulent Shear Flows, Penn. State Univ.*, p. 11.23.
- ZAMAN, K. B. M. Q. & HUSSAIN, A. K. M. F. 1980 *J. Fluid Mech.* **101**, 449.